Experiments on Tunneling and Correlations

E. Y. Andrei, S. Yücel, and L. Menna
Department of Physics, Rutgers University, Piscataway, New Jersey 08855-0849
(Received 26 August 1991)

We observed tunneling in a system of interacting electrons confined to a two-dimensional layer. The effects of correlations on the tunneling were studied by varying the electron density from the single-particle limit to the highly correlated Wigner-crystal regime. For low densities the tunneling is well described by a model in which the interactions are represented by an effective potential.

PACS numbers: 73.40.Gk, 73.20.Dx

Tunneling is one of the most ubiquitous manifestations of quantum mechanics and has been invoked in the explanation of such diverse phenomena as the formation of the Universe or the decay of nuclei. When applied to a single particle crossing a known potential barrier, the concept of tunneling is well understood. In most real systems, however, interparticle interactions alter the tunneling process and the problem becomes more complex. It is therefore of considerable interest to devise a system in which single-particle tunneling through a known potential barrier can be observed and that also allows a gradual "dialing-in" of interactions.

The layer of electrons trapped at the liquid-helium–vacuum interface is such a system. A potential well formed at the interface restricts their motion in the z direction while their motion in a plane parallel to the helium surface is free. By applying an electric field in the z direction the potential can be transformed into a finite barrier through which an electron can escape. During the escape it interacts with the other electrons in the layer and the escape rates are modified by electron-electron correlations. The correlations can be tuned by varying the electron density (*in situ*) over several orders of magnitude ranging from the dilute single-electron limit $\Gamma < 50$ to the highly correlated Wigner-crystal regime $\Gamma > 127$, where $\Gamma = (\pi n_s)^{1/2} e^2/k_B T$ measures the correlation strength and n_s is the electronic density [1]. The system is extremely clean, and the potential barrier and all interactions are well characterized and tunable. As a result the tunneling does not involve unknown parameters arising from random impurities, unspecified boundaries, and undefined local potential barriers, as it does in most other systems studied so far: electron microscopes, quantum wells, alpha decay, etc. Of course, thermal activation provides another escape mechanism which becomes dominant at high temperatures [2–4]. In previous attempts to detect tunneling in this system, Goodkind *et al.* [3] observed a crossover from thermally activated to temperature-independent escape rates. These rates, however, were 50 orders of magnitude faster than calculated tunneling rates [3,5,6] and attempts to interpret them in terms of tunneling have so far been unsuccessful.

In this Letter we report the first observation of tunneling of electrons through a barrier formed above the liquid-helium surface. We explored the dependence of the tunneling rates on the electron density and found that below a critical density n_c, the effect of correlations can be described by an effective potential theory [2]. We show that at low temperatures, $T \leq 200$ mK, tunneling is the dominant escape mechanism, while at higher temperatures thermal activation takes over.

Our experiment monitors the decay of the electronic density following the creation of a potential barrier through which they can escape. We measure the escape rate as a function of electron density, barrier height, and temperature. The experimental cell consists of two parallel metallic plates separated by a distance $D = 2.5$ mm, between which the helium substrate supports the electron layer. The helium thickness, $h = 1.28$ mm, is determined to within 15 μm from the capacitance between the top and bottom plates. The helium temperature, $30 \leq T \leq 450$ mK, is measured with a carbon thermometer in the top plate. The electrons are generated with a tungsten filament located behind a grid in the top plate. They are directed towards the helium surface by ramping the voltage between the top and bottom plates, V_t, to the value $V_t^0 = -2\pi |e| n_s (h/\epsilon + d)$ where $d = D - h$, and $\epsilon = 1.057$ is the dielectric constant of liquid helium. An 18-mm-diam guard ring that is kept at a negative voltage $V_g < V_t^0$ confines the electrons within the area of a disk whose radius and density profile are uniquely determined [7] by the geometry of the cell and the values of V_t and V_g. A more precise determination of n_s is obtained with a swept radio-frequency (rf) spectroscopy technique. The rf spectrum consists of a series of screened plasmon resonances at the normal mode frequencies of the electron disk [7]:

$$\omega_{\mu,\nu}^2 = \frac{4\pi n_s e^2 k_{\mu,\nu}}{m[\coth(k_{\mu,\nu} d) + \epsilon \coth(k_{\mu,\nu} h)]},$$

where the wave vectors $k_{\mu,\nu}$ are quantized by the boundary condition of vanishing radial current at the edge of the disk, $\mu = 1,2,\ldots$; $\nu = 0,1,\ldots$; m is the electronic mass. From this spectrum, which typically consists of seven or more well-resolved resonances, we can determine changes in n_s to an accuracy of $\sim 0.01\%$ in the range 2×10^6 to 2×10^8 cm^{-2}.

To initiate the escape we apply a voltage pulse V_t^b between the top and bottom plates which creates the potential barrier. In the work described here the rise time and duration of the pulses were typically ~ 30 and ~ 250 μsec, respectively. The pulses were repeated until most of the electrons disappeared. The rf spectra were recorded in between pulses with the top plate and guard ring voltages sufficiently negative to prevent further escape.

Throughout the experiments described here these voltages were kept at the values $V_t^m = -15$ V and $V_g = -42$ V. From these spectra and from the density profile defined by V_t^m and V_g we obtained N_s and ΔN_s, the total number of electrons in the disk and of electrons lost, respectively. The escape rate is thus $W(n_s) = \Delta N_s / \tau N_s$, where ΔN_s is determined from values of N_s before and after the pulse and n_s is the average density *during* the pulse which we calculate from V_t^b, V_g. The parameters of the pulse were chosen so that its duration, $\tau \geq 0.1$ msec, was shorter than the time to lose 1% of the electrons. The rise time of the pulse ~ 30 μsec was chosen so as not to cause additional electron loss due to the high-frequency transients it introduces. Indeed such effects were observed for much shorter rise times ≤ 1 μsec. We also studied the pulse length dependence of the escape rates by repeating the same experiment with various pulses in the range of 100 $\mu\text{sec} \leq \tau \leq 20$ min and found that for sufficiently low densities, $n_s < n_c$, they are independent of τ. The spectrum itself and our determination of N_s are not sensitive to the electronic temperature, but the escape rate may be.

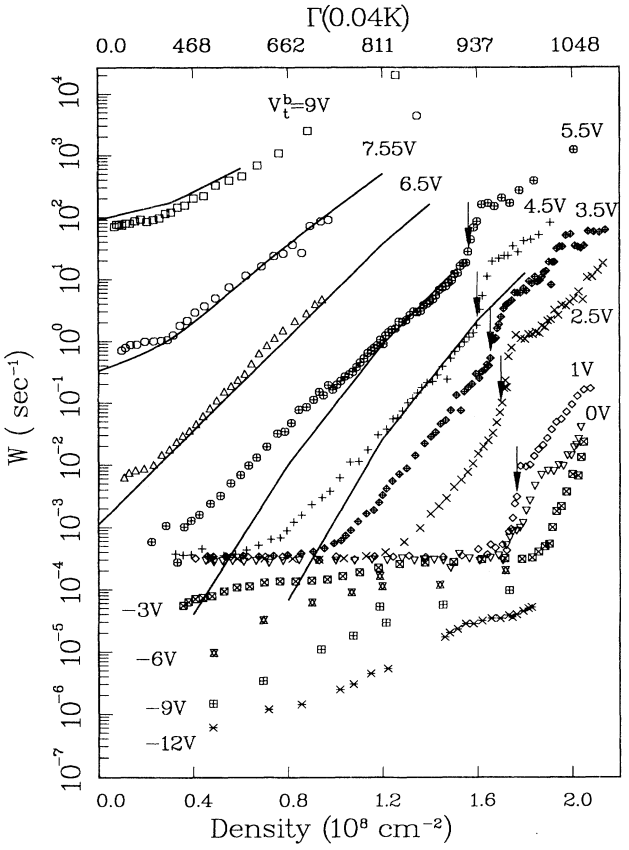

FIG. 1. Density dependence of the escape rates W at $T = 40$ mK for a series of fixed top plate voltages V_t^b. The solid lines are linear interpolations between calculated tunneling rates at discrete values of n_s, for $V_t^b = 9$, 7.5, 6.5, 5.5, and 4.5 V. Vertical arrows indicate the positions of n_c for $V_t^b = 5.5$, 4.5, 3.5, 2.5, and 1 V.

We observed that recording the rf spectrum during the pulse causes an increase in the escape rates, proportional to the time spent sweeping through a resonance and to the power level of the rf source. Off resonance the escape rates are insensitive to comparable levels of rf power. Our procedure avoids these heating effects since the rf spectra are recorded in between pulses when the electrons are pressed into the helium and the electron ripplon interaction, which is the main thermalization mechanism, is enhanced.

In Fig. 1 we display the density dependence of the escape rates at 40 mK, for a series of fixed values of V_t^b. Most of the density range explored at this temperature is in the Wigner-crystal phase as indicated by the values of Γ. We distinguish between three regimes where the escape is qualitatively different: In region A, characterized by $W > 4\times10^{-4}$ sec^{-1} and $n_s < n_c$, with n_c indicated by vertical arrows, the escape depends strongly on n_s and V_t^b but is independent of τ. Below we show that the escape in this regime can be attributed to tunneling. In region B, where $W < 4\times10^{-4}$ sec^{-1}, the rates are independent of n_s and V_t^b, until $V_t^b < 0$, when they start displaying a very weak dependence on the experimental parameters. In region C, where $n_s > n_c$, the rates are strongly dependent on τ. For $\tau \geq 0.4$ msec the number of electrons lost in this region increased precipitously with pulse length and the rates were not measurable until the density dropped below n_c. When measured with shorter pulses, $\tau \leq 150$ μsec, the pulse length dependence became very

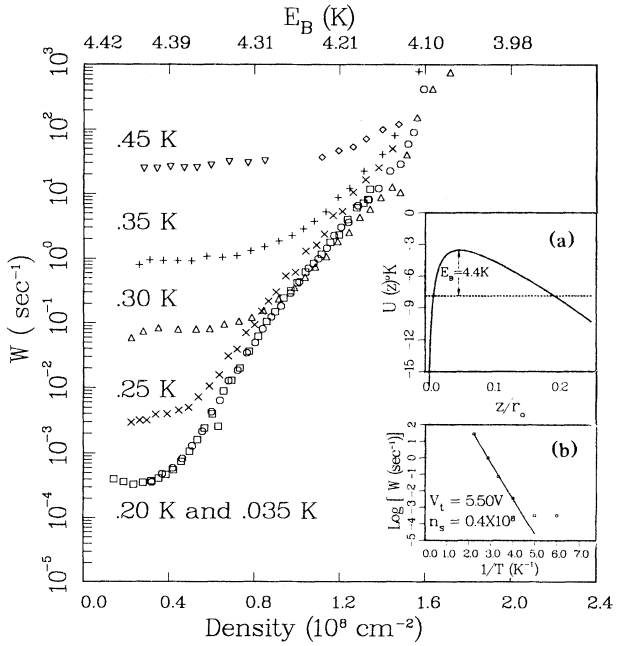

FIG. 2. Temperature dependence of electron escape rates for $V_t^b = 5.5$ V. Inset (a) illustrates the CHM barrier and metastable state for $V_t^b = 5.5$ V and $n_s = 0.4\times10^8$ cm^{-2}. In inset (b) we plot the measured thermal activation rates (□), together with the two-parameter fit by Eq. (3), solid line.

weak and the rates exhibited an abrupt 1 order of magnitude increase at $n_s = n_c$.

In Fig. 2 we illustrate the temperature dependence of the escape rate curves for $V_t^b = 5.5$ V. The temperature-dependent rates do not become measurable until $T > 200$ mK, when they start dominating the escape at the lowest densities. We observe no signature of the liquid-solid transition in the escape rates.

To interpret our results we must first determine the potential barrier. Its precise form depends on the effect of correlations on the escaping electron. We will adopt an approach [2,3] which assumes that the correlations can be described by an effective potential $U_c(z)$:

$$U_c(z) = |e|\mathcal{E}_c \times \begin{cases} z^2/2r_0, & z < r_0, \\ z - r_0/2, & z \geq r_0, \end{cases} \quad (1)$$

where $\mathcal{E}_c = -2\pi|e|n_s$. This implies that for distances $z \leq r_0$ the electron interacts with the correlation hole, of radius $r_0 = 1.38(\pi n_s)^{-1/2}$, that is left in the continuous charge sheet after the escape. At larger distances the hole closes and the potential is that of a continuous charge sheet: $U_c(z) = e(\mathcal{E}_i + \mathcal{E}_c)z$, where $\mathcal{E}_i = \mathcal{E}_c(h/\epsilon - d)/(h/\epsilon + d)$ arises from positive image charges induced on the top and bottom plates. The helium surface is close to the electrical midpoint of our cell, so $h = \epsilon d$, and $\mathcal{E}_i \simeq 0$. Its actual position can vary slightly between runs and introduces a correction to $U_c(z)$. In this model which we refer to as the correlation-hole model (CHM) the potential energy of the escaping electron is

$$U(z) = -\frac{Qe^2}{z} - V_t^b|e|\frac{z}{h/\epsilon + d} + U_c(z), \quad (2)$$

where the first term is due to the attraction of the polarized helium substrate, $Q = (\epsilon - 1)/4(\epsilon + 1)$, and the second term is introduced by V_t^b, whose sign determines whether the applied potential causes the barrier to become narrower (positive) or wider (negative). It is this term that allows experimental control over the parameters of the barrier: For $V_t^b \leq V_t^0$ the electron is bound in a Rydberg state while for $V_t^b > V_t^0$ (note that $V_t^0 < 0$) a finite potential barrier is formed whose size decreases as V_t^b increases. To obtain the tunneling rates through this barrier we calculate numerically the energy and lifetime of the electron in the resonant states of the CHM Hamiltonian with a Breit-Wigner technique which was described in detail elsewhere [5]. All the relevant parameters in this calculation, n_s, h, and V_t^b, were directly measured in the experiment. The small error in the helium level $\Delta h = \pm 15$ μm introduces an uncertainty in $U_c(z)$ that may cause at most a 1 order of magnitude variation in the escape rates. In our calculations we have chosen a single value of h, within the stated error, to fit the data presented in Fig. 1. The energy spectrum obtained from this calculation consists of a series of metastable states whose number decreases with increasing V_t^b, until at sufficiently small barriers only one metastable state remains. In this regime the escape becomes significantly simpler, since it involves no intermediate states which may cause instabilities that complicate the process [8]. The tunneling rate W is obtained from the resonance width, the binding energy of the electron E_B is the difference between the maximum of the potential and the energy of this state, and the barrier width Δz is the distance between its turning points. There is no simple analytic expression for E_B and Δz to replace the numerical solutions, but an approximate form may be used for $V_t^b > 0$ (pulling fields) in two limits:

$$E_B \sim \tfrac{1}{2} + \tfrac{3}{2}\mathcal{E}_p - \begin{cases} 2|\mathcal{E}_p|^{1/2}, & |\mathcal{E}_c| \ll \mathcal{E}_p, \\ \tfrac{3}{2}(|\mathcal{E}|_c/r_0)^{1/3}, & \mathcal{E}_p \ll |\mathcal{E}_c|, \end{cases}$$

$$\Delta z \sim (r_0\mathcal{E}_p/\mathcal{E}_c)[(1 + \mathcal{E}_c/r_0\mathcal{E}_p^2)^{1/2} - 1] - 2, \quad |\mathcal{E}_c|, \mathcal{E}_p \ll 1,$$

where $\mathcal{E}_p = V_t^b/(h/\epsilon + d)$ is the electric field above the electron layer arising from the applied voltage. Here all quantities are expressed in scaled atomic units: energy, $Q^2e^2/a_B = 15.2$ K; distance, $a_B/Q = 76.1$ Å; and electric field, $eQ^2/a_B = 1727.2$ V/cm. In our experiments $20 \leq \Delta z \leq 80$, $0.2 \leq E_B < 1$, and $70 \leq r_0 \leq 700$.

The measured escape rates could be due to tunneling or to activation above the barrier. We identify the tunneling regime with the temperature-independent data that are fitted by the calculated rates in the CHM. In this regime, region A, the model predicts a narrow barrier, $\Delta z < 0.5r_0$, with a single metastable state. The calculated tunneling rates [5], plotted in Fig. 1, follow closely the measured ones. The single-particle tunneling rates corresponding to the zero-density limit of this calculation are in remarkably good agreement with the low-density limit of the measured rates for the largest pulling fields $V_t^b > 7$ V where the ratio $\Delta z/r_0$ is smallest. In this limit, the barrier width is much smaller than the electron spacing and, as expected, single-particle behavior becomes dominant.

Another useful way of presenting the data is to plot the escape rates as a function of E_B as in Fig. 3. Along lines

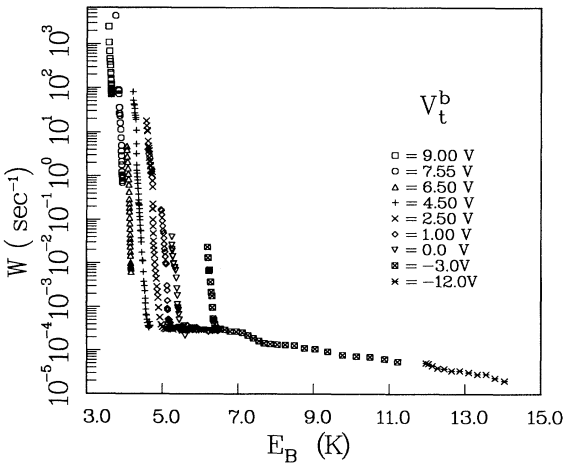

FIG. 3. Escape rates W (data of Fig. 1) as a function of barrier height E_B at $T = 40$ mK for a series of voltages V_t^b.

of fixed E_B the rates in region A vary by several orders of magnitude. As expected of tunneling, these rates depend on both barrier height and width. They are temperature independent until taken over by thermally activated rates. By contrast with tunneling the thermally activated rates shown in Fig. 2 can be identified from their slow variation with density and from their exponential variation with temperature. The temperature-dependent rates start dominating the escape for $T > 200$ mK at the lowest densities and with increasing temperature they take over at successively higher densities. At a fixed temperature their slow variation with density can be understood in terms of a slow barrier-height variation over the density regime studied as predicted by the CHM (upper abscissa in Fig. 2). In inset (b) of Fig. 2 we show the temperature dependence of the thermally activated rates at $n_s = 0.4 \times 10^8$ cm^{-2} together with a two-parameter fit by an expression for the theoretically calculated thermal activation rates induced by electron-ripplon interactions [9]:

$$W = C\left(\frac{m}{\hbar^3\sigma}\right)T^2 E_B\left(1+\frac{3k_BT}{E_B}\right)\exp\left(-\frac{E_B}{k_BT}\right). \quad (3)$$

Here σ is the helium surface tension and $C = 0.354$ was obtained from a first-principles calculation in the uncorrelated limit $r_0 = 0$. The best-fit value obtained for the barrier height, $E_B = 4.4 \pm 0.1$ K, coincides with the value $E_B = 4.4$ K calculated in the CHM. The smaller value obtained for the prefactor, $C = 0.071 \pm 0.004$, could be attributed to a correlation-induced slowdown of the rates. For $W < 10^{-4}$ sec^{-1} a sharp deviation from this behavior indicates the crossover into region B.

The CHM is very successful in describing the escape in region A, where the barrier is mostly determined by the external field. As V_t^b decreases the barrier becomes larger causing a slowdown in the tunneling rates. A prominent feature of the escape in this region is the appearance of a lower bound on the rates at 4×10^{-4} sec^{-1}, which is independent of n_s and of V_t^b for $4.5\ \text{V} \geq V_t^b \geq 0$ V and only weakly dependent on them for $V_t^b < 0$. These features, which characterize the escape in region B, are not consistent with the escape mechanisms discussed so far. In Fig. 3 the escape for $E_B \geq 6$ K, region B, clearly separates away from the tunneling regime. In region B the rates are single valued in E_B and seem to converge to a straight line whose slope could be interpreted in terms of an energy of 3.5 ± 0.4 K. The origin of such an energy scale and how it would affect the escape is yet unknown. So far we have ruled out vibrations, a tilted helium surface, and cosmic muons.

To compare our results to those of Ref. [3] we have plotted in Fig. 4 the escape rate versus V_t^b at $n_s = 0.8 \times 10^8$ cm^{-2}, together with calculated tunneling rates. For $V_t^b \geq 4$ V the rates are in region A and the calculated rates follow closely the measured ones. At lower V_t^b, region B, they break away abruptly from the tunneling curve. The temperature-independent rates of Ref. [3], indicated on this plot by triangles [10], are clearly situated in region B.

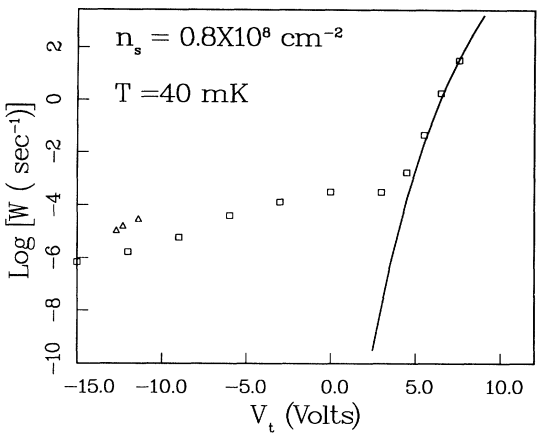

FIG. 4. Escape rates W (data of Fig. 1) as a function of the top plate voltage V_t^b for the electronic density 0.8×10^8 cm^{-2} and temperature 40 mK. □, rates measured in this work; △, rates reported in Ref. [3]; solid line, calculated rates in the correlation-hole model.

In region C where $n_s \geq n_c(V_t^b)$ we observe an instability signaled by the onset of a nonlinear dependence on τ. More detailed studies, which will be discussed elsewhere, indicate that the locus of the instability corresponds to a fixed value of total energy acquired by electrons that impact the top plate, $E = (|\mathcal{E}_c| + |\mathcal{E}|_p)(D-h) = 20 \pm 1$ eV, and seems to involve electronic excitations in the helium atoms coating the top plate.

We thank C. Chaleil-Heyer, J. Verrier, and W. Henderson for technical help, N. Andrei, A. Ruckenstein, Y. Vilk, and F. I. B. Williams for useful discussion, and NSF (DMR 90-24964 and DMR 90-22252) for support.

[1] For a review, see E. Y. Andrei, F. I. B. Williams, C. D. Glattli, and G. Deville, in *The Physics of Low Dimensional Semiconductors* (Plenum, New York, 1991).

[2] Y. Iye, K. Kono, K. Kajita, and W. Sasaki, J. Low Temp. Phys. **38**, 293 (1980); K. Kono, K. Kajita, S. Kobayashi, and W. Sasaki, J. Low Temp. Phys. **46**, 195 (1982); also H. Totsuji, Phys. Rev. A **17**, 399 (1978).

[3] J. M. Goodkind, G. F. Saville, A. Ruckenstein, and P. M. Platzman, Phys. Rev. B **38**, 8788 (1988).

[4] V. A. Buntar, V. N. Grigoriev, O. I. Kirichek, Yu. Z. Kovdrya, Y. P Monarkha, and S. Sokolov, J. Low Temp. Phys. **79**, 323 (1990).

[5] S. Yücel and E. Y. Andrei, Phys. Rev. B **42**, 2088 (1990).

[6] M. A. Azbel and P. M. Platzman, Phys. Rev. Lett. **65**, 1376 (1990).

[7] C. D. Glattli, E. Y. Andrei, G. Deville, J. Poitrenaud, and F. I. B. Williams, Phys. Rev. Lett. **54**, 1710 (1985).

[8] G. F. Saville, J. M. Goodkind, and P. M. Platzman, Phys. Rev. Lett. **61**, 1237 (1988).

[9] S. Nagano, S. Ichimaru, H. Totsuji, and N. Itoh, Phys. Rev. B **19**, 2449 (1979).

[10] The points of Ref. [3] were taken at a higher density and temperature than those presented in Fig. 4.